

Supplementary material for

A cloud screening algorithm for ground-based sun photometry using all-sky images and deep transfer learning

Eric A. Wendt¹, Bonne Ford², and John Volckens¹

¹Department of Mechanical Engineering, Colorado State University, Fort Collins, Colorado, USA, 80523

²Department of Atmospheric Science, Colorado State University, Fort Collins, Colorado, USA, 80523

Contents of this file

Text S1

Figures S1 to S12

Table S1

Introduction

Text S1 describes the development of the all-sky imaging module used to collect NCASI images. Text S2 describes in detail the preprocessing steps used to prepare all-sky images to interface with deep transfer learning models. Figure S1 is a photograph of the imaging module used to collect NCASI images. Figure S2 gives example images from each data set and each category (cirrus, clear, cloud). Figure S3 gives example results of the preprocessing algorithm. Figures S4-S9 give confusion matrices for models not featured in the main text. Figures S10-S12 give all the images misclassified by model 7. Table S1 gives a cost summary for the images module. Tables S2 and S3 give accuracy results for three-class and two-class classification problems, respectively.

Text S1. We designed a prototype all-sky-imaging module using relatively low-cost, and commercially available components. The camera included an image sensor (Sony, IMX477-AACK-C, Minato City, Tokyo, Japan) and integrated circuitry for simple interfacing with the Raspberry Pi 4B. We achieved a 180° field of view using a fisheye lens (Arducam Technology Co., Limited, M25170H12, Hong Kong), and adequate sunlight attenuation by layering three, 3-stop, neutral density filters (Kodak, 1964741, Rochester, New York, USA) between the image sensor element and the lens. A photograph of the module and its associated componentry is provided in Fig. S1.

We used a Raspberry Pi 4B with 4 GB of RAM (Raspberry Pi Foundation, Cambridge, United Kingdom) as the processing unit and the Raspberry Pi HQ Camera Module (Raspberry Pi Foundation, SC0261, Cambridge, United Kingdom) as the imaging unit. The camera included an image sensor (Sony, IMX477-AACK-C, Minato City, Tokyo, Japan) and integrated circuitry for simple interfacing with the Raspberry Pi 4B. We achieved a 180° field of view using a fisheye lens (Arducam Technology Co., Limited, M25170H12, Hong Kong), and adequate sunlight attenuation by layering three, 3-stop, neutral density filters (Kodak, 1964741, Rochester, New York, USA) between the image sensor element and the lens. This configuration had the effect of reducing the image sensor exposure by a factor of 512. The Raspberry Pi 4B was powered with a 5 V, 4 Ah Lithium Polymer battery. We housed the electrical components in an electrical enclosure (Polycase, YQ-080804, Avon, Ohio, USA) and cut a circular hole in the lid to expose the image sensor to the sky. The cost of goods to produce a single prototype was 282.48 USD. A summary of component costs is provided in Table S1.

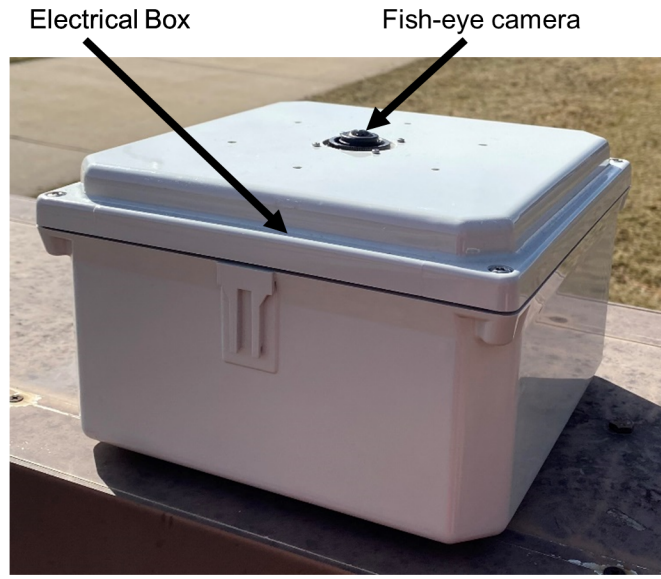
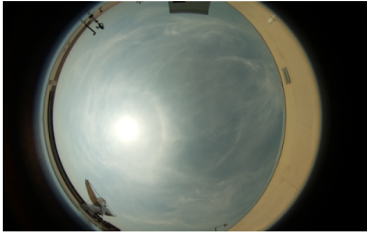
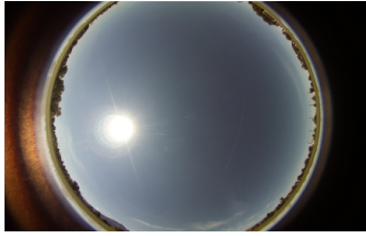


Figure S1. Photograph of NCASI imaging module.

NCASI Cirrus



NCASI Clear



NCASI Cloud



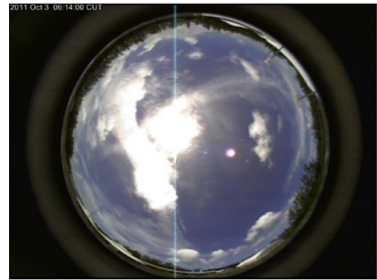
METCRAX-II Cirrus



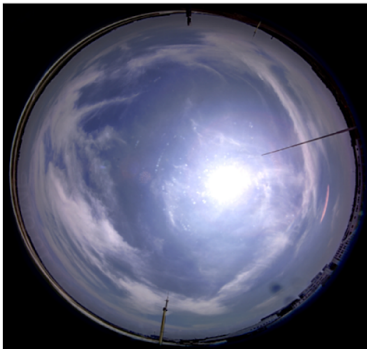
METCRAX-II Clear



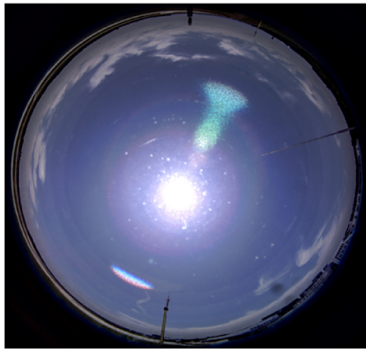
METCRAX-II Cloud



WSISEG Cirrus



WSISEG Clear



WSISEG Cloud

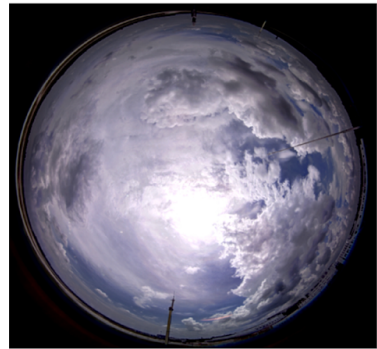


Figure S2. Example images from NCASI, METACRAX-II, and WSISEG for cirrus, clear, and cloud designations

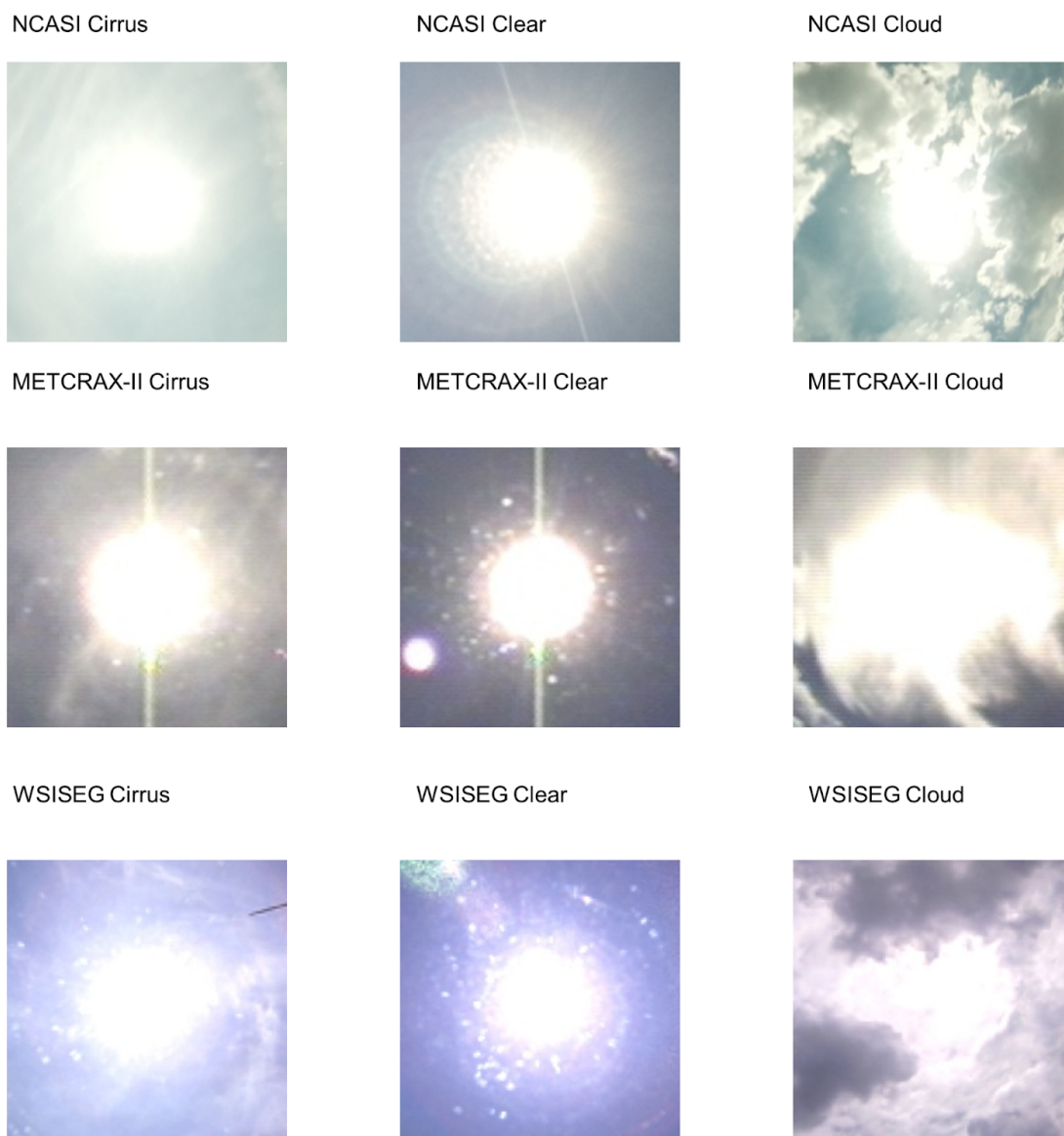


Figure S3. Example pre-processed images from NCASI, METACRAX-II, and WSISEG for cirrus, clear, and cloud designations.

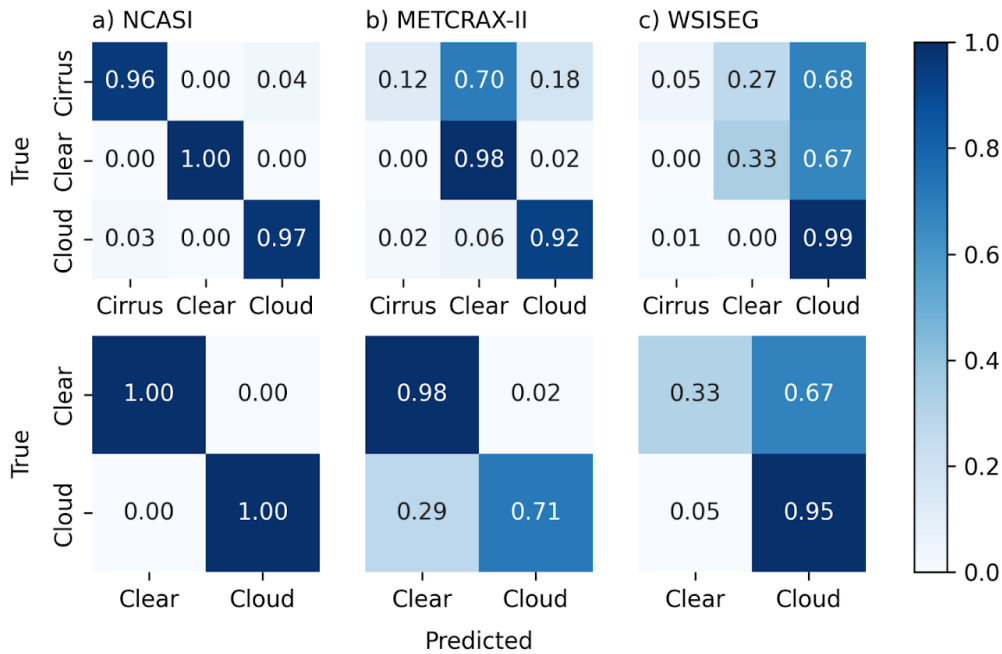


Figure S4. Top row: three-class confusion matrices for transfer learning model trained on NCASI training data set (model 1). a) Results on NCASI testing data set. b) Results on METCRAX-II testing data set. c) Results on WSISEG testing data set. Bottom row: two-class confusion matrices for transfer learning model trained on NCASI training data set (model 1). a) Results on NCASI testing data set. b) Results on METCRAX-II testing data set. c) Results on WSISEG testing data set.

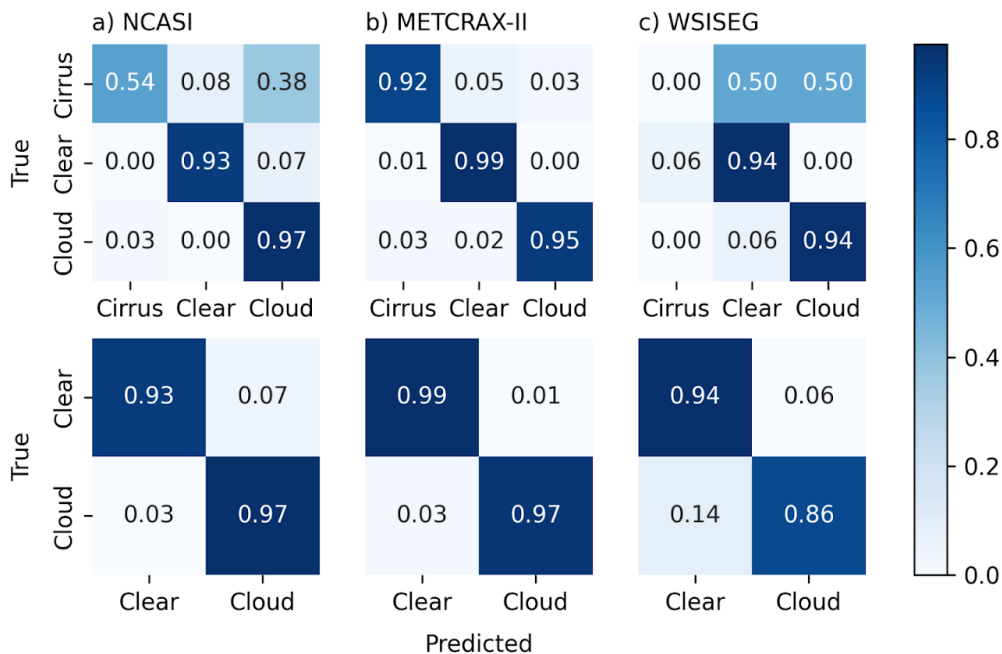


Figure S5. Top row: three-class confusion matrices for transfer learning model trained on METCRAX-II training data set (model 2). a) Results on NCASI testing data set. b) Results on METCRAX-II testing data set. c) Results on WSISEG testing data set. Bottom row: two-class confusion matrices for transfer

learning model trained on METCRAX-II training data set (model 2). a) Results on NCASI testing data set. b) Results on METCRAX-II testing data set. c) Results on WSISEG testing data set.

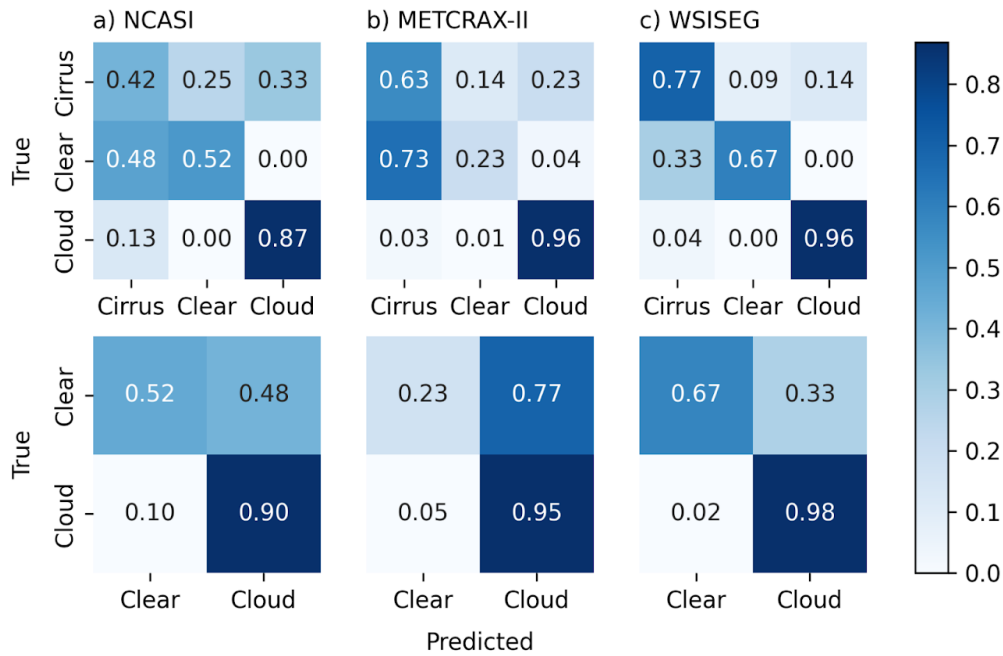


Figure S6. Top row: three-class confusion matrices for transfer learning model trained on WSISEG training data set (model 3). a) Results on NCASI testing data set. b) Results on METCRAX-II testing data set. c) Results on WSISEG testing data set. Bottom row: two-class confusion matrices for transfer learning model trained on WSISEG training data set (model 3). a) Results on NCASI testing data set. b) Results on METCRAX-II testing data set. c) Results on WSISEG testing data set.

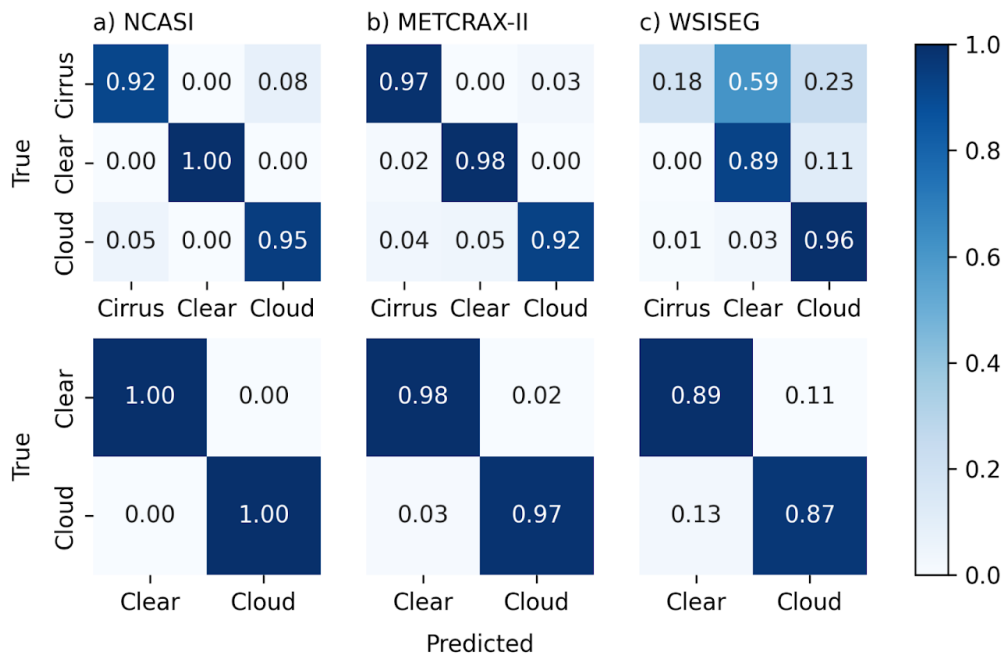


Figure S7. Top row: three-class confusion matrices for transfer learning model trained on NCASI and

METCRAX-II training data sets (model 4). a) Results on NCASI testing data set. b) Results on METCRAX-II testing data set. c) Results on WSISEG testing data set. Bottom row: two-class confusion matrices for transfer learning model trained on NCASI and METCRAX-II training data sets (model 4). a) Results on NCASI testing data set. b) Results on METCRAX-II testing data set. c) Results on WSISEG testing data set.

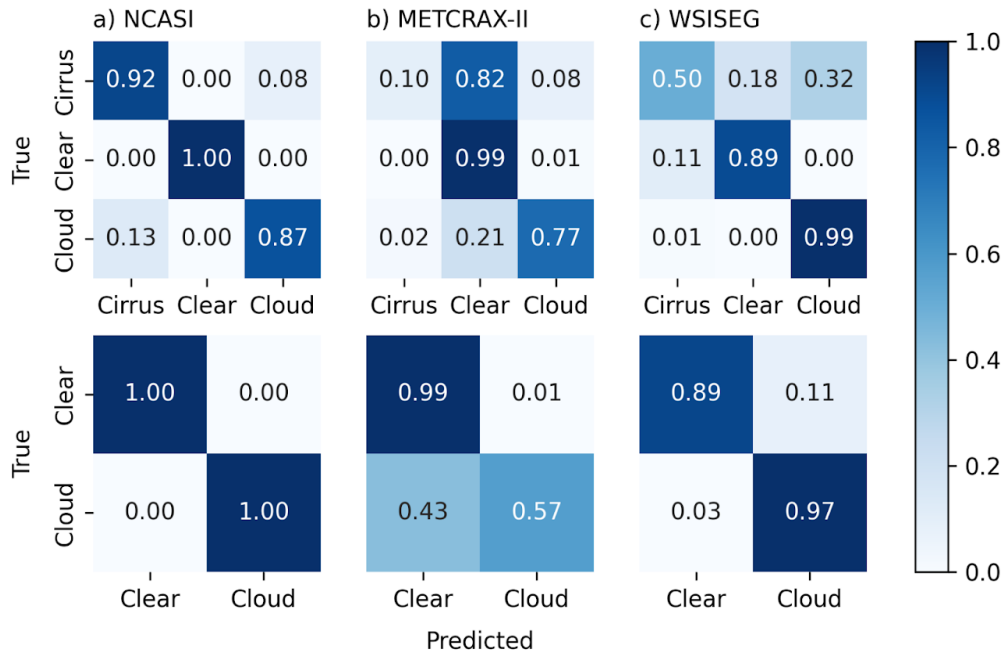


Figure S8. Top row: three-class confusion matrices for transfer learning model trained on NCASI and WSISEG training data sets (model 5). a) Results on NCASI testing data set. b) Results on METCRAX-II testing data set. c) Results on WSISEG testing data set. Bottom row: two-class confusion matrices for transfer learning model trained on NCASI and WSISEG training data sets (model 5). a) Results on NCASI testing data set. b) Results on METCRAX-II testing data set. c) Results on WSISEG testing data set.

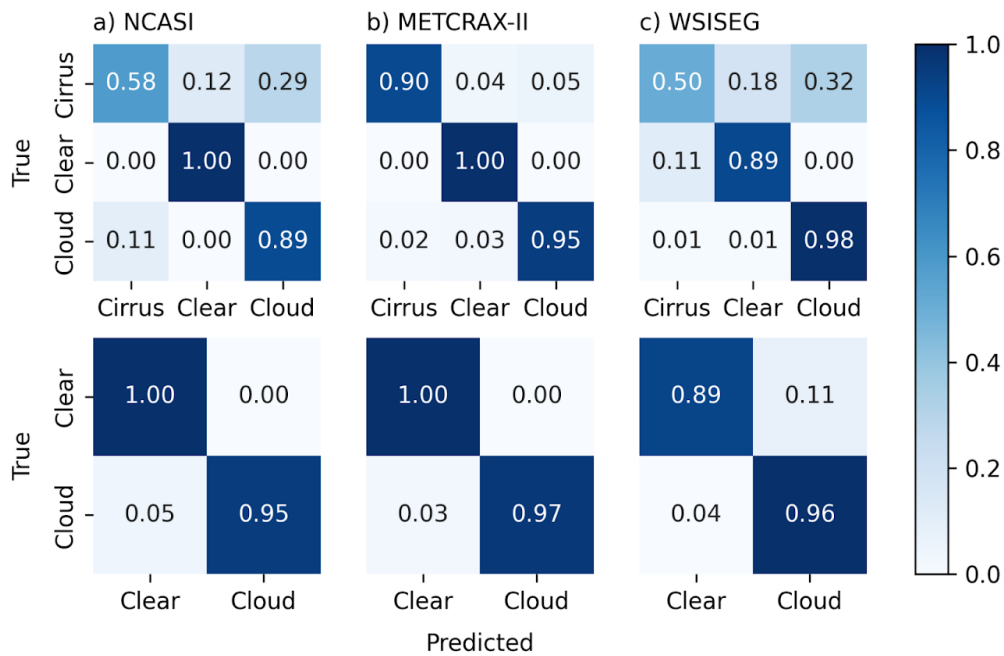


Figure S9. Top row: three-class confusion matrices for transfer learning model trained on METCRAX-II and WSISEG training data sets (model 6). a) Results on NCASI testing data set. b) Results on METCRAX-II testing data set. c) Results on WSISEG testing data set. Bottom row: two-class confusion matrices for transfer learning model trained on METCRAX-II and WSISEG training data sets (model 6). a) Results on NCASI testing data set. b) Results on METCRAX-II testing data set. c) Results on WSISEG testing data set.



Figure S10. Misclassified images on NCASI testing data set for the model trained on NCASI, METCRAX-II, and WSISEG data sets (model 7).



Figure S11. Misclassified images on METCRAX-II testing data set for the model trained on NCASI, METCRAX-II, and WSISEG data sets (model 7).

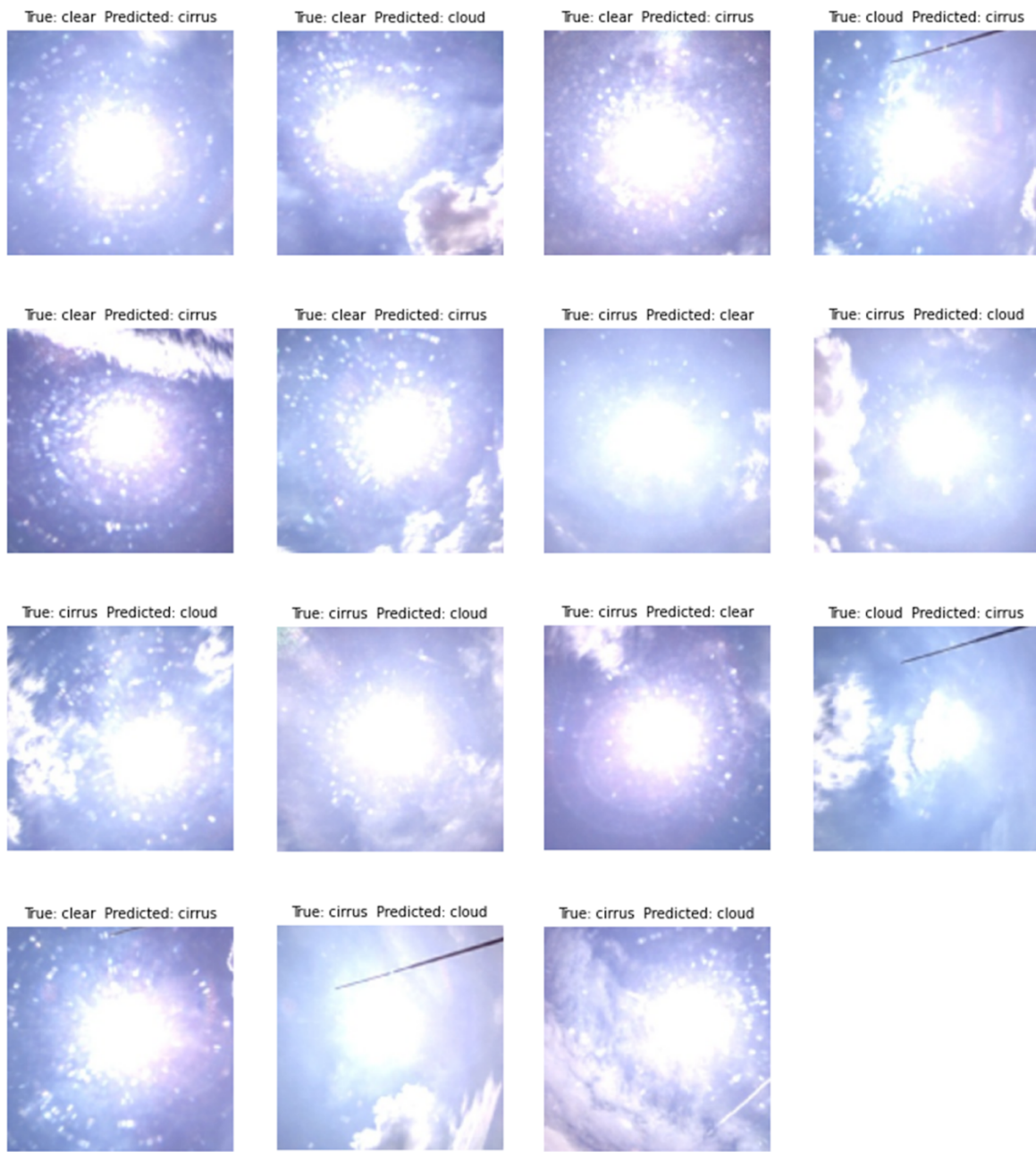


Figure S12. Misclassified images on WSISEG testing data set for the model trained on NCASI, METCRAX-II, and WSISEG data sets (model 7).

Table S1. Component costs of imaging module

Component	Manufacturer	Part Number	Cost (USD)
Raspberry Pi 4 Model B 4 GB	Raspberry Pi Foundation	Raspberry Pi 4B/4GB	55.00
Raspberry Pi HQ Camera Module	Raspberry Pi Foundation	SC0261	50.00
Arducam M12 Fisheye Lens	Arducam Technology Co., Limited	M25170H12	9.99
Neutral Density Optical Gelatin Wratten Filter (75 mm ×75 mm)	Kodak	1964741	97.50
Electrical Box	Polycase	YQ-0808804-13	55.00
Battery Pack for Raspberry Pi, 4000mAh	Yapears	5647469919	14.99

Total Cost: 282.48 USD